

Accessing GPDs through the exclusive photoproduction of a photon-meson pair with a large invariant mass

3DPartons Week

Saad Nabeebaccus



Gluodynamics

October 28, 2022

Based on works with S. Wallon, L. Szymanowski, B. Pire, R. Boussarie,
G. Duplančić, K. Passek-Kumerički

Introduction

GPDs: Deeply virtual Compton Scattering (DVCS)

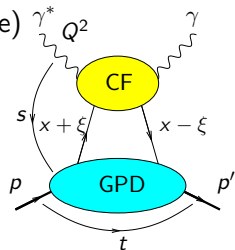
DVCS: exclusive process (non forward amplitude)

Fourier transf.: $t \leftrightarrow$ impact parameter

$(x, \xi, t) \Rightarrow$ 3-dimensional structure

Coefficient Function (hard) \otimes **Generalized Parton Distribution** (soft)

[Müller et al. '91 - '94; Radyushkin '96; Ji '97]

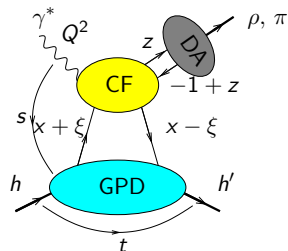


Introduction

GPDs: Deeply Virtual Meson Production (DVMP)

DVMP: γ replaced by ρ, π, \dots

GPD (soft) \otimes CF (hard) \otimes Distribution Amplitude (soft)



[Collins, Frankfurt, Strikman '97; Radyushkin '97]

proofs valid only for some restricted cases

Quark GPDs at twist 2 [Diehl]

without helicity flip (chiral-even Γ matrices): 4 chiral-even GPDs:
(Note: $\Delta = p' - p$)

$$\begin{aligned} F^q &= \frac{1}{2} \int \frac{dz^-}{2\pi} e^{ixP^+z^-} \langle p' | \bar{q}(-\frac{1}{2}z) \gamma^+ q(\frac{1}{2}z) | p \rangle \Big|_{z^+=0, z_\perp=0} \\ &= \frac{1}{2P^+} \left[H^q(x, \xi, t) \bar{u}(p') \gamma^+ u(p) + E^q(x, \xi, t) \bar{u}(p') \frac{i \sigma^{+\alpha} \Delta_\alpha}{2m} u(p) \right], \end{aligned}$$

Quark GPDs at twist 2 [Diehl]

without helicity flip (chiral-even Γ matrices): 4 chiral-even GPDs:
(Note: $\Delta = p' - p$)

$$\begin{aligned} F^q &= \frac{1}{2} \int \frac{dz^-}{2\pi} e^{ixP^+z^-} \langle p' | \bar{q}(-\frac{1}{2}z) \gamma^+ q(\frac{1}{2}z) | p \rangle \Big|_{z^+=0, z_\perp=0} \\ &= \frac{1}{2P^+} \left[H^q(x, \xi, t) \bar{u}(p') \gamma^+ u(p) + E^q(x, \xi, t) \bar{u}(p') \frac{i\sigma^{+\alpha} \Delta_\alpha}{2m} u(p) \right], \end{aligned}$$

$$\begin{aligned} \tilde{F}^q &= \frac{1}{2} \int \frac{dz^-}{2\pi} e^{ixP^+z^-} \langle p' | \bar{q}(-\frac{1}{2}z) \gamma^+ \gamma_5 q(\frac{1}{2}z) | p \rangle \Big|_{z^+=0, z_\perp=0} \\ &= \frac{1}{2P^+} \left[\tilde{H}^q(x, \xi, t) \bar{u}(p') \gamma^+ \gamma_5 u(p) + \tilde{E}^q(x, \xi, t) \bar{u}(p') \frac{\gamma_5 \Delta^+}{2m} u(p) \right]. \end{aligned}$$

Introduction

Quark GPDs: twist 2 Chiral-even

Quark GPDs at twist 2 [Diehl]

without helicity flip (chiral-even Γ matrices): 4 chiral-even GPDs:
(Note: $\Delta = p' - p$)

$$\begin{aligned} F^q &= \frac{1}{2} \int \frac{dz^-}{2\pi} e^{ixP^+z^-} \langle p' | \bar{q}(-\frac{1}{2}z) \gamma^+ q(\frac{1}{2}z) | p \rangle \Big|_{z^+=0, z_\perp=0} \\ &= \frac{1}{2P^+} \left[H^q(x, \xi, t) \bar{u}(p') \gamma^+ u(p) + E^q(x, \xi, t) \bar{u}(p') \frac{i\sigma^{+\alpha} \Delta_\alpha}{2m} u(p) \right], \end{aligned}$$

$$\begin{aligned} \tilde{F}^q &= \frac{1}{2} \int \frac{dz^-}{2\pi} e^{ixP^+z^-} \langle p' | \bar{q}(-\frac{1}{2}z) \gamma^+ \gamma_5 q(\frac{1}{2}z) | p \rangle \Big|_{z^+=0, z_\perp=0} \\ &= \frac{1}{2P^+} \left[\tilde{H}^q(x, \xi, t) \bar{u}(p') \gamma^+ \gamma_5 u(p) + \tilde{E}^q(x, \xi, t) \bar{u}(p') \frac{\gamma_5 \Delta^+}{2m} u(p) \right]. \end{aligned}$$

$$H^q \xrightarrow{\xi=0, t=0} \text{PDF } q \qquad \tilde{H}^q \xrightarrow{\xi=0, t=0} \text{polarized PDF } \Delta q$$

Introduction

Quark GPDs: twist 2 Chiral-odd

with helicity flip (chiral-odd Γ matrices): 4 chiral-odd GPDs:

$$\begin{aligned} & \frac{1}{2} \int \frac{dz^-}{2\pi} e^{ixP^+z^-} \langle p' | \bar{q}(-\frac{1}{2}z) i\sigma^{+i} q(\frac{1}{2}z) | p \rangle \Big|_{z^+=0, z_\perp=0} \\ &= \frac{1}{2P^+} \bar{u}(p') \left[H_T^q i\sigma^{+i} + \tilde{H}_T^q \frac{P^+ \Delta^i - \Delta^+ P^i}{m^2} \right. \\ & \quad \left. + E_T^q \frac{\gamma^+ \Delta^i - \Delta^+ \gamma^i}{2m} + \tilde{E}_T^q \frac{\gamma^+ P^i - P^+ \gamma^i}{m} \right] u(p), \end{aligned}$$

with helicity flip (chiral-odd Γ matrices): 4 chiral-odd GPDs:

$$\begin{aligned} & \frac{1}{2} \int \frac{dz^-}{2\pi} e^{ixP^+z^-} \langle p' | \bar{q}(-\frac{1}{2}z) i\sigma^{+i} q(\frac{1}{2}z) | p \rangle \Big|_{z^+=0, z_\perp=0} \\ &= \frac{1}{2P^+} \bar{u}(p') \left[H_T^q i\sigma^{+i} + \tilde{H}_T^q \frac{P^+\Delta^i - \Delta^+P^i}{m^2} \right. \\ & \quad \left. + E_T^q \frac{\gamma^+\Delta^i - \Delta^+\gamma^i}{2m} + \tilde{E}_T^q \frac{\gamma^+P^i - P^+\gamma^i}{m} \right] u(p), \end{aligned}$$

$$H_T^q \xrightarrow{\xi=0, t=0} \text{quark transversity PDFs } \delta q$$

Note: $\tilde{E}_T^q(x, -\xi, t) = -\tilde{E}_T^q(x, \xi, t)$

Why consider a gamma-meson pair?

Understanding transversity

- ▶ Transverse spin content of the proton:

$$\begin{array}{l} |\uparrow\rangle_{(x)} \quad \sim \quad |\rightarrow\rangle + |\leftarrow\rangle \\ |\downarrow\rangle_{(x)} \quad \sim \quad |\rightarrow\rangle - |\leftarrow\rangle \\ \text{spin along } x \quad \quad \quad \text{helicity states} \end{array}$$

- ▶ Observables which are sensitive to helicity flip thus give access to transversity PDFs. Poorly known.

Why consider a gamma-meson pair?

Understanding transversity

- ▶ Transverse spin content of the proton:

$$\begin{array}{l} |\uparrow\rangle_{(x)} \quad \sim \quad |\rightarrow\rangle + |\leftarrow\rangle \\ |\downarrow\rangle_{(x)} \quad \sim \quad |\rightarrow\rangle - |\leftarrow\rangle \\ \text{spin along } x \quad \quad \quad \text{helicity states} \end{array}$$

- ▶ Observables which are sensitive to helicity flip thus give access to transversity PDFs. Poorly known.
- ▶ Transversity GPDs are completely unknown experimentally.
- ▶ For massless (anti)particles, chirality = (-)helicity
- ▶ Transversity GPDs can thus be accessed through **chiral-odd Γ** matrices.

Why consider a gamma-meson pair?

Understanding transversity

- ▶ Transverse spin content of the proton:

$$\begin{array}{lcl} |\uparrow\rangle_{(x)} & \sim & |\rightarrow\rangle + |\leftarrow\rangle \\ |\downarrow\rangle_{(x)} & \sim & |\rightarrow\rangle - |\leftarrow\rangle \\ \text{spin along } x & & \text{helicity states} \end{array}$$

- ▶ Observables which are sensitive to helicity flip thus give access to transversity PDFs. Poorly known.
- ▶ Transversity GPDs are completely unknown experimentally.
- ▶ For massless (anti)particles, chirality = (-)helicity
- ▶ Transversity GPDs can thus be accessed through **chiral-odd Γ** matrices.
- ▶ Since (in the massless limit) QCD and QED are chiral-even ($\gamma^\mu, \gamma^\mu\gamma^5$), **the chiral-odd quantities ($1, \gamma^5, [\gamma^\mu, \gamma^\nu]$) which one wants to measure should appear in pairs.**

Why consider a gamma-meson pair?

Can we probe transversity GPDs in meson production?

- ▶ the leading DA (twist 2) of ρ_T is **chiral-odd** ($\sigma^{\mu\nu}$ coupling)

Why consider a gamma-meson pair?

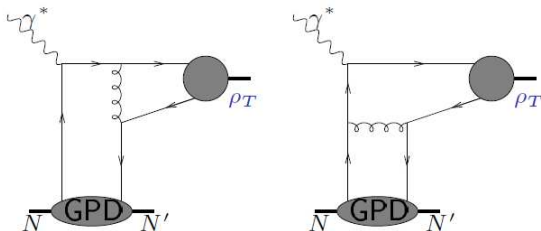
Can we probe transversity GPDs in meson production?

- ▶ the leading DA (twist 2) of ρ_T is **chiral-odd** ($\sigma^{\mu\nu}$ coupling)
- ▶ unfortunately $\gamma^* N \rightarrow \rho_T N' = 0$, since such a process would require a helicity transfer of 2 from a photon. [Diehl, Gousset, Pire], [Collins, Diehl]

Why consider a gamma-meson pair?

Can we probe transversity GPDs in meson production?

- ▶ the leading DA (twist 2) of ρ_T is **chiral-odd** ($\sigma^{\mu\nu}$ coupling)
- ▶ unfortunately $\gamma^* N \rightarrow \rho_T N' = 0$, since such a process would require a helicity transfer of 2 from a photon. [Diehl, Gousset, Pire], [Collins, Diehl]
- ▶ lowest order diagrammatic argument:



$$\gamma^\alpha [\gamma^\mu, \gamma^\nu] \gamma_\alpha = 0$$

Why consider a gamma-meson pair?

Go to higher twist?

- ▶ This vanishing only occurs at twist 2
- ▶ At twist 3 this process does not vanish [Ahmad, Goldstein, Liuti], [Goloskokov, Kroll]

Why consider a gamma-meson pair?

Go to higher twist?

- ▶ This vanishing only occurs at twist 2
- ▶ At twist 3 this process does not vanish [Ahmad, Goldstein, Liuti], [Goloskokov, Kroll]
- ▶ However processes involving twist 3 DAs may face problems with factorisation (end-point singularities)
can be made safe in the high-energy k_T -factorisation approach
[Anikin, Ivanov, Pire, Szymanowski, Wallon]

Why consider a gamma-meson pair?

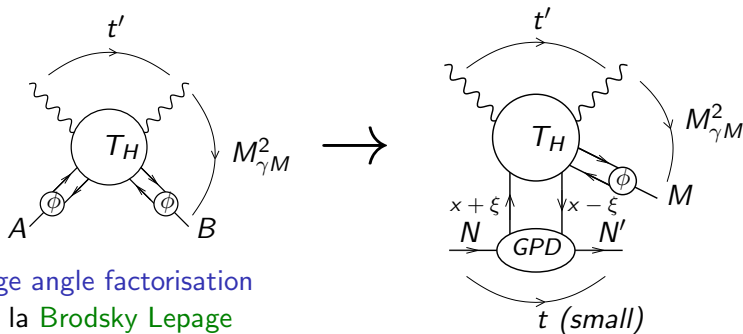
A convenient alternative solution

- ▶ Circumvent this using 3-body final states [Ivanov, Pire, Szymanowski, Teryaev], [Enberg, Pire, Szymanowski], [El Beiyad, Pire, Segond, Szymanowski, Wallon]
- ▶ Consider the process $\gamma N \rightarrow \gamma MN'$, $M = \text{meson}$. Collinear factorisation of the amplitude at large $M_{\gamma M}^2$.

Why consider a gamma-meson pair?

A convenient alternative solution

- ▶ Circumvent this using 3-body final states [Ivanov, Pire, Szymanowski, Teryaev], [Enberg, Pire, Szymanowski], [El Beiyad, Pire, Segond, Szymanowski, Wallon]
- ▶ Consider the process $\gamma N \rightarrow \gamma M N'$, $M = \text{meson}$. Collinear factorisation of the amplitude at large $M_{\gamma M}^2$.



large angle factorisation
à la Brodsky Lepage

Why consider a gamma-meson pair?

Is factorisation justified?

- ▶ Recently, factorisation has been proved for the process $MN \rightarrow \gamma\gamma N'$ by Qiu, Yu [2205.07846].

Why consider a gamma-meson pair?

Is factorisation justified?

- ▶ Recently, factorisation has been proved for the process $MN \rightarrow \gamma\gamma N'$ by Qiu, Yu [2205.07846].
- ▶ Requires large p_T .

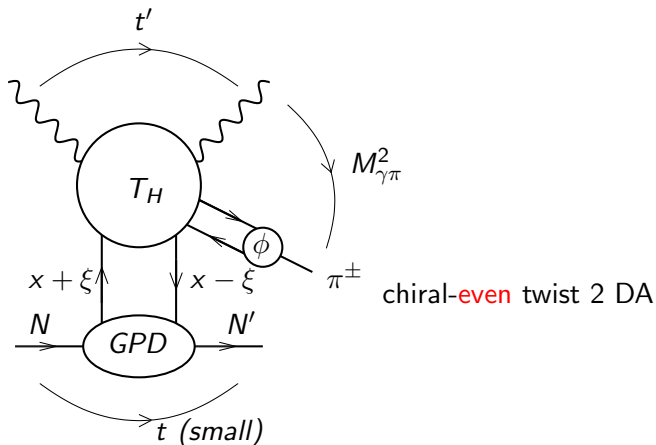
Why consider a gamma-meson pair?

Is factorisation justified?

- ▶ Recently, factorisation has been proved for the process $MN \rightarrow \gamma\gamma N'$ by Qiu, Yu [2205.07846].
- ▶ Requires large p_T .
- ▶ In fact, NLO computation has been performed for $\gamma N \rightarrow \gamma\gamma N'$ by Grocholski et al. [2110.00048]. \implies See Lech's talk

Why consider a gamma-meson pair?

Chiral-even GPDs using $\pi^\pm \gamma$ production

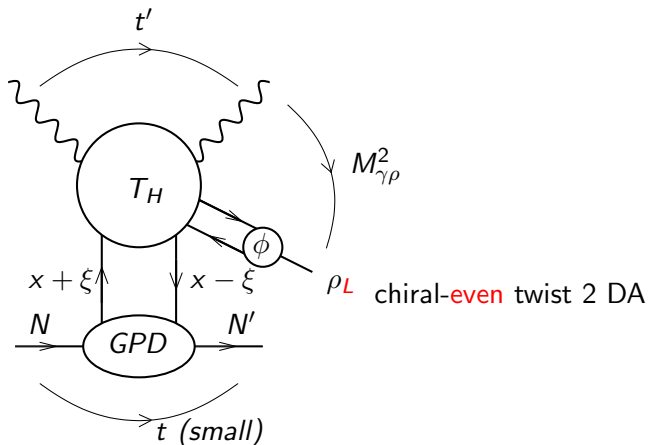


chiral-even twist 2 GPD

[G. Duplanić, K. Passek-Kumerički, B. Pire, L. Szymanowski, S. Wallon]

Why consider a gamma-meson pair?

Chiral-even GPDs using $\rho_L \gamma$ production

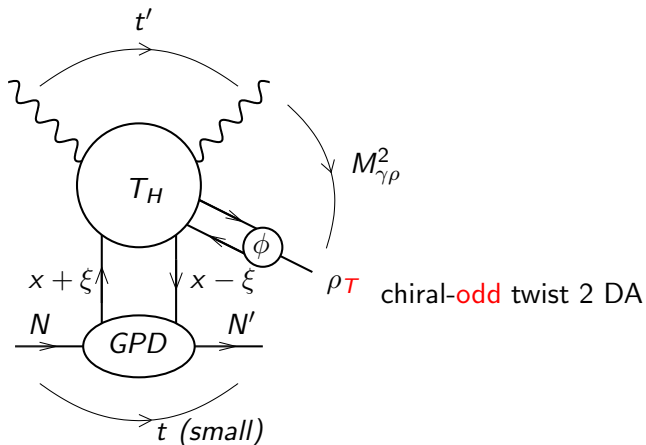


chiral-even twist 2 GPD

[R. Boussarie, B. Pire, L. Szymanowski, S. Wallon]

Why consider a gamma-meson pair?

Chiral-odd GPDs using $\rho_T \gamma$ production



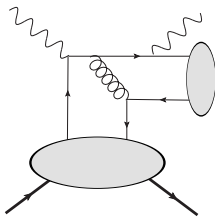
chiral-odd twist 2 GPD

[R. Boussarie, B. Pire, L. Szymanowski, S. Wallon]

Why consider a gamma-meson pair?

Chiral-odd GPDs using $\rho T \gamma$ production

How does it work?



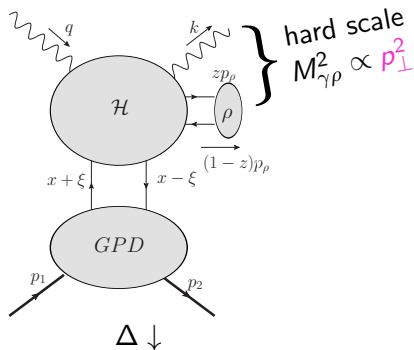
Typical non-zero diagram for a **transverse** ρ meson

the σ matrices (from either the DA or the GPD) do not kill it anymore!

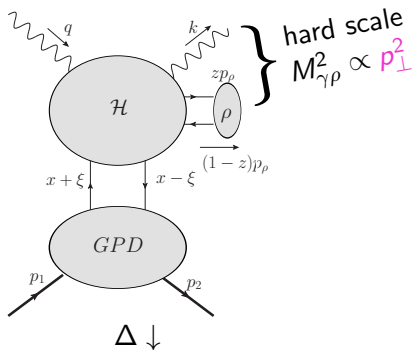
Computation

Kinematics

$$\gamma(q) + N(p_1) \rightarrow \gamma(k) + \rho(p_\rho, \varepsilon_\rho) + N'(p_2)$$



$$\gamma(q) + N(p_1) \rightarrow \gamma(k) + \rho(p_\rho, \varepsilon_\rho) + N'(p_2)$$



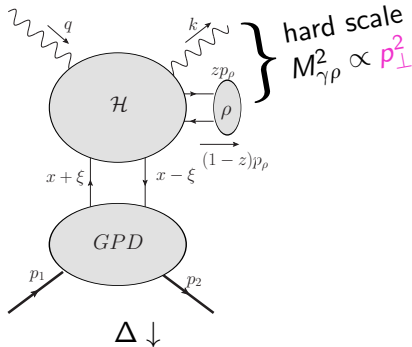
Useful Mandelstam variables:

$$t = (p_2 - p_1)^2$$

$$u' = (p_\rho - q)^2$$

$$t' = (k - q)^2$$

$$\gamma(q) + N(p_1) \rightarrow \gamma(k) + \rho(p_\rho, \varepsilon_\rho) + N'(p_2)$$



Useful Mandelstam variables:

$$t = (p_2 - p_1)^2$$

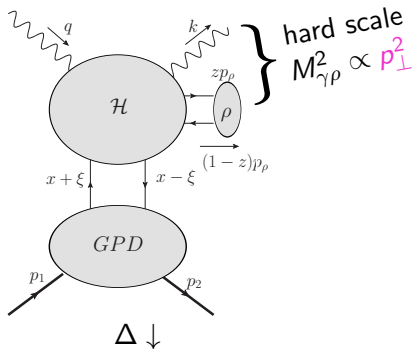
$$u' = (p_\rho - q)^2$$

$$t' = (k - q)^2$$

► Factorisation requires:

$$-u' > 1 \text{ GeV}^2, \quad -t' > 1 \text{ GeV}^2 \text{ and } (-t)_{\min} \leq -t \leq .5 \text{ GeV}^2$$

$$\gamma(q) + N(p_1) \rightarrow \gamma(k) + \rho(p_\rho, \varepsilon_\rho) + N'(p_2)$$



Useful Mandelstam variables:

$$t = (p_2 - p_1)^2$$

$$u' = (p_\rho - q)^2$$

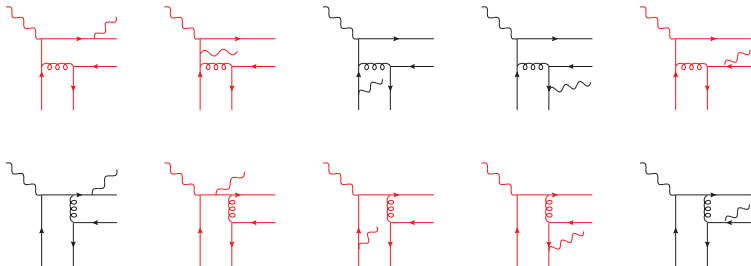
$$t' = (k - q)^2$$

- Factorisation requires:

$$-u' > 1 \text{ GeV}^2, \quad -t' > 1 \text{ GeV}^2 \quad \text{and} \quad (-t)_{\min} \leq -t \leq .5 \text{ GeV}^2$$

- Cross-section differential in $(-u')$ and $M_{\gamma\rho}^2$, and evaluated at $(-t) = (-t)_{\min}$.

A total of 20 diagrams to compute



- ▶ The other half can be deduced by $q \leftrightarrow \bar{q}$ (anti)symmetry depending on C -parity in t -channel
- ▶ Red diagrams cancel in the chiral-odd case

Computation

Parametrising the GPDs: 2 scenarios for polarized PDFs

We parameterise the GPDs in terms of *double distributions*
(*Radyushkin-type parametrisation*)

We parameterise the GPDs in terms of *double distributions* (*Radyushkin-type parametrisation*)

For **polarized** PDFs (and hence **transversity** PDFs), two scenarios are proposed for the parameterization:

- ▶ “**standard**” scenario, with flavor-symmetric light sea quark and antiquark distributions.
- ▶ “**valence**” scenario with a completely flavor-asymmetric light sea quark densities.

- ▶ We take the simplistic **asymptotic** form of the DAs

$$\phi_{\pi}(z) = \phi_{\rho\parallel}(z) = \phi_{\rho\perp}(z) = 6z(1-z).$$

- ▶ We also investigate the effect of using a **holographic** DA (**preliminary**):

$$\phi_{\text{hol}}(z) = \frac{8}{\pi} \sqrt{z(1-z)}.$$

- ▶ We take the simplistic **asymptotic** form of the DAs

$$\phi_{\pi}(z) = \phi_{\rho\parallel}(z) = \phi_{\rho\perp}(z) = 6z(1-z).$$

- ▶ We also investigate the effect of using a **holographic** DA (**preliminary**):

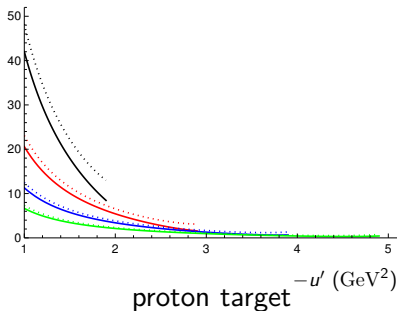
$$\phi_{\text{hol}}(z) = \frac{8}{\pi} \sqrt{z(1-z)}.$$

Suggested by AdS/QCD correspondence [**Brodsky, de Teramond**], dynamical chiral symmetry breaking on the light-front [**Shi et al.**], and recent lattice results. [**Gao et al.**]

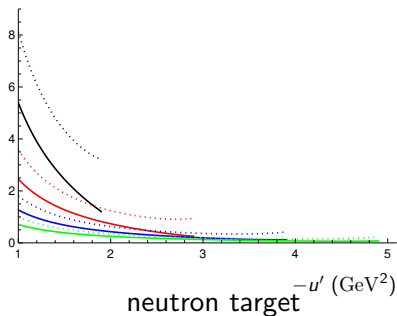
Results

Fully-differential cross-sections: ρ_L^0 (Chiral even)

$$\frac{d\sigma_{\text{even}}}{dM_{\gamma\rho}^2 d(-u') d(-t)} \quad (\text{pb} \cdot \text{GeV}^{-6})$$



$$\frac{d\sigma_{\text{even}}}{dM_{\gamma\rho}^2 d(-u') d(-t)} \quad (\text{pb} \cdot \text{GeV}^{-6})$$



$S_{\gamma N} = 20 \text{ GeV}^2$, at $-t = (-t)_{\text{min}}$, asymptotical DA

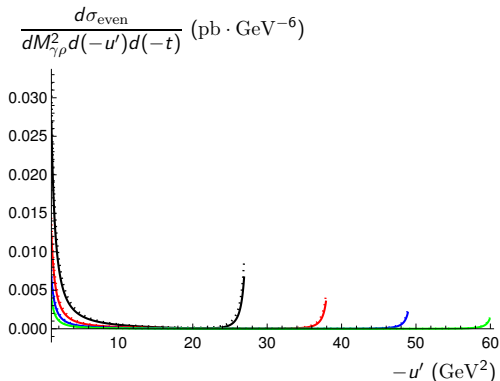
$$M_{\gamma\rho}^2 = 3, 4, 5, 6 \text{ GeV}^2$$

dotted: "standard" model

solid: "valence" model

Results (Preliminary)

Fully-differential cross-sections: ρ_L^0 (Chiral even)



$S_{\gamma N} = 200 \text{ GeV}^2$, at $-t = (-t)_{\min}$, asymptotical DA, proton target

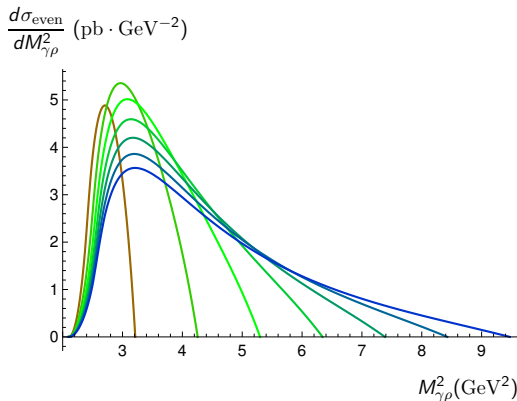
$$M_{\gamma\rho}^2 = 28, 39, 50, 61 \text{ GeV}^2$$

dotted: "standard" model

solid: "valence" model

Results

Single differential cross-section: ρ_L^0 (Chiral even)

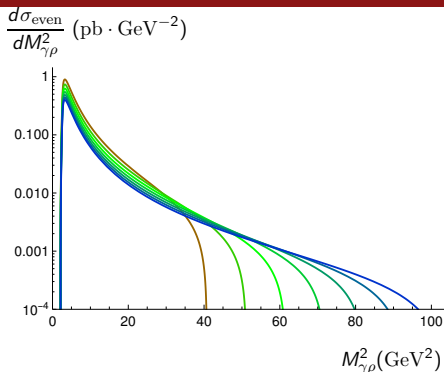


proton target, “valence” scenario, asymptotical DA

$$S_{\gamma N} = 8, 10, 12, 14, 16, 18, 20 \text{ GeV}^2 \text{ (typical JLab kinematics)}$$

Results (Preliminary)

Single differential cross-section: ρ_L^0 (Chiral even)



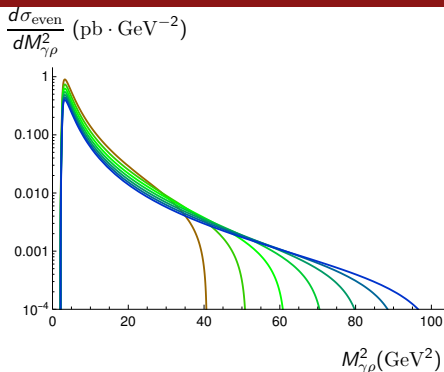
proton target, “valence” scenario, asymptotical DA

$$S_{\gamma N} = 80, 100, 120, 140, 160, 180, 200 \text{ GeV}^2$$

(typical COMPASS kinematics)

Results (Preliminary)

Single differential cross-section: ρ_L^0 (Chiral even)



proton target, "valence" scenario, asymptotical DA

$$S_{\gamma N} = 80, 100, 120, 140, 160, 180, 200 \text{ GeV}^2$$

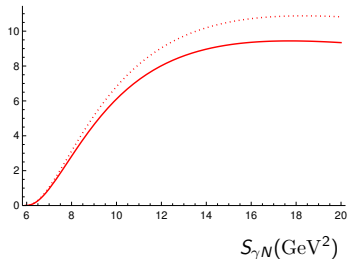
(typical COMPASS kinematics)

Peak *always* at low $M_{\gamma M}^2 \implies$ Importance sampling needed for higher $S_{\gamma N}$!

Results

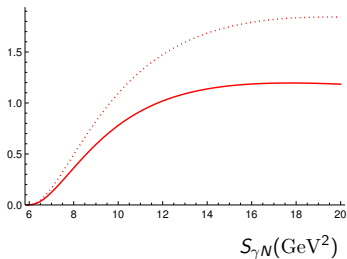
Integrated cross-section: Valence vs Standard: ρ_L^0 (Chiral even)

σ_{even} (pb)



proton target

σ_{even} (pb)



neutron target

Asymptotical DA

solid: "valence" scenario

dotted: "standard" one

Results

Integrated cross-section: Mapping procedure for different values of $S_{\gamma N}$

To obtain distribution in $S_{\gamma N}$, we exploit non-trivial mapping between 1 set of data at a fixed $S_{\gamma N}$ to other values $\tilde{S}_{\gamma N}$ *lower* than it.

Results

Integrated cross-section: Mapping procedure for different values of $S_{\gamma N}$

To obtain distribution in $S_{\gamma N}$, we exploit non-trivial mapping between 1 set of data at a fixed $S_{\gamma N}$ to other values $\tilde{S}_{\gamma N}$ *lower* than it.

$$\tilde{M}_{\gamma M}^2 = M_{\gamma M}^2 \frac{\tilde{S}_{\gamma N} - M_N^2}{S_{\gamma N} - M_N^2},$$
$$- \tilde{u}' = \frac{\tilde{M}_{\gamma M}^2}{M_{\gamma M}^2} (-u').$$

Results

Integrated cross-section: Mapping procedure for different values of $S_{\gamma N}$

To obtain distribution in $S_{\gamma N}$, we exploit non-trivial mapping between 1 set of data at a fixed $S_{\gamma N}$ to other values $\tilde{S}_{\gamma N}$ *lower* than it.

$$\tilde{M}_{\gamma M}^2 = M_{\gamma M}^2 \frac{\tilde{S}_{\gamma N} - M_N^2}{S_{\gamma N} - M_N^2},$$
$$- \tilde{u}' = \frac{\tilde{M}_{\gamma M}^2}{M_{\gamma M}^2} (-u').$$

Implementing **importance sampling** \implies careful consideration of the various limits involved are needed.

Results

Integrated cross-section: Mapping procedure for different values of $S_{\gamma N}$

To obtain distribution in $S_{\gamma N}$, we exploit non-trivial mapping between 1 set of data at a fixed $S_{\gamma N}$ to other values $\tilde{S}_{\gamma N}$ *lower* than it.

$$\tilde{M}_{\gamma M}^2 = M_{\gamma M}^2 \frac{\tilde{S}_{\gamma N} - M_N^2}{S_{\gamma N} - M_N^2},$$
$$- \tilde{u}' = \frac{\tilde{M}_{\gamma M}^2}{M_{\gamma M}^2} (-u').$$

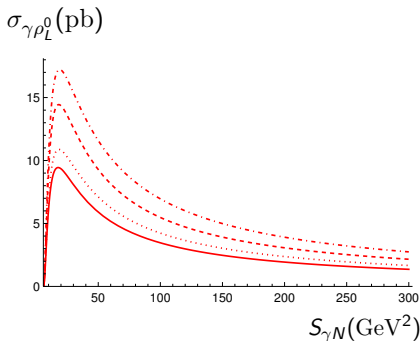
Implementing **importance sampling** \implies careful consideration of the various limits involved are needed.

Mapping possible since **different** sets of $(S_{\gamma N}, M_{\gamma M}^2, -u')$ correspond to the **same** (α, ξ) .

$$\alpha = \frac{-u'}{M_{\gamma M}^2}, \quad \xi = \frac{M_{\gamma M}^2}{2(S_{\gamma N} - M_N^2) - M_{\gamma M}^2}.$$

Results (Preliminary)

Fully differential cross-section: Holographic vs Asymptotical DA: ρ_L^0 (Chiral-even)

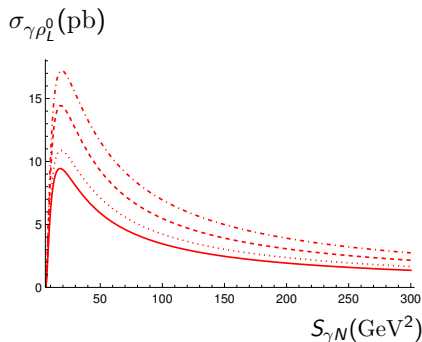


Dashed: Holographic DA non-dashed: Asymptotical DA

Dotted: standard scenario non-dotted: valence scenario

Results (Preliminary)

Fully differential cross-section: Holographic vs Asymptotical DA: ρ_L^0 (Chiral-even)



Dashed: Holographic DA non-dashed: Asymptotical DA

Dotted: standard scenario non-dotted: valence scenario

\implies DA type has sizable effect, larger than the one due to uncertainties on polarized PDFs

Results (Preliminary)

Polarisation Asymmetries of incoming photon

Results (Preliminary)

Polarisation Asymmetries of incoming photon

- ▶ Circular asymmetry = 0 (for unpolarised target).

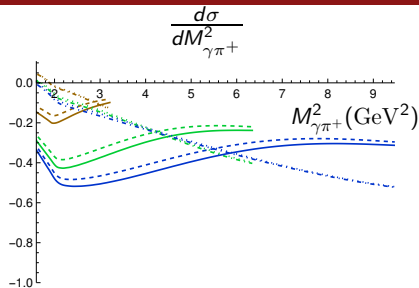
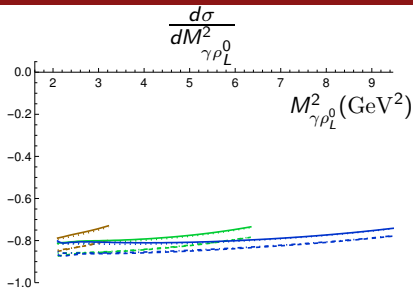
Results (Preliminary)

Polarisation Asymmetries of incoming photon

- ▶ Circular asymmetry = 0 (for unpolarised target).
- ▶ Linear asymmetry = $\frac{d\sigma_x - d\sigma_y}{d\sigma_x + d\sigma_y}$, where x is the direction defined by p_\perp (direction of outgoing photon in the transverse plane).
- ▶ **Kleiss-Sterling** spinor techniques used to obtain expressions.

Results (Preliminary)

Polarisation Asymmetries of incoming photon



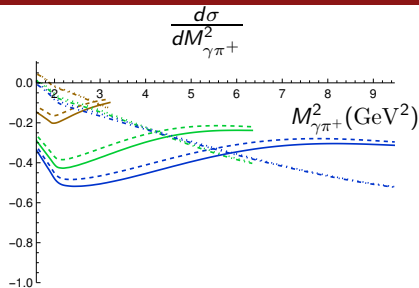
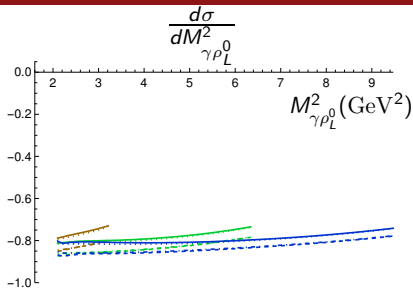
Dashed: Holographic DA non-dashed: Asymptotical DA

Dotted: standard scenario non-dotted: valence scenario

► $S_{\gamma N} = 8, 14, 20$ GeV²

Results (Preliminary)

Polarisation Asymmetries of incoming photon



Dashed: Holographic DA non-dashed: Asymptotical DA

Dotted: standard scenario non-dotted: valence scenario

► $S_{\gamma N} = 8, 14, 20$ GeV²

► ρ_L^0 can distinguish between DA model, while π^+ (and π^-) can distinguish between GPD model (valence vs standard).

Prospects at experiments

Counting rates: JLab

Good statistics: For example, at [JLab Hall B](#):

- ▶ untagged incoming $\gamma \Rightarrow$ [Weizsäcker-Williams](#) distribution

Good statistics: For example, at [JLab Hall B](#):

- ▶ untagged incoming $\gamma \Rightarrow$ **Weizsäcker-Williams** distribution
- ▶ with an expected luminosity of $\mathcal{L} = 100 \text{ nb}^{-1}\text{s}^{-1}$, for 100 days of run:
 - ρ_L^0 (on p) : $\approx 2.4 \times 10^5$
 - ρ_T^0 (on p) : $\approx 7.5 \times 10^3$ (Chiral-odd)
 - ρ_L^+ : $\approx 1.4 \times 10^5$
 - π^+ : $\approx 1.8 \times 10^5$

At COMPASS:

- ▶ Taking a luminosity of $\mathcal{L} = 0.1 \text{ nb}^{-1}\text{s}^{-1}$, and 300 days of run,
 - ρ_L^0 (on p) : $\approx 1.2 \times 10^3$
 - ρ_L^+ : $\approx 7.4 \times 10^2$
 - π^+ : $\approx 4.5 \times 10^2$

At COMPASS:

- ▶ Taking a luminosity of $\mathcal{L} = 0.1 \text{ nb}^{-1}\text{s}^{-1}$, and 300 days of run,
 - ρ_L^0 (on p) : $\approx 1.2 \times 10^3$
 - ρ_L^+ : $\approx 7.4 \times 10^2$
 - π^+ : $\approx 4.5 \times 10^2$
- ▶ Lower numbers due to low luminosity (factor of 10^3 less than JLab!)

Prospects at experiments (Preliminary)

Counting rates: EIC

- ▶ At the future EIC, with an expected integrated luminosity of 10 fb^{-1} (about 100 times smaller than JLab):
 - ρ_L^0 (on p) : $\approx 2.4 \times 10^4$
 - ρ_L^+ : $\approx 1.5 \times 10^4$
 - π^+ : $\approx 1.3 \times 10^4$

Prospects at experiments (Preliminary)

Counting rates: EIC

- ▶ At the future **EIC**, with an expected integrated luminosity of 10 fb^{-1} (about 100 times smaller than JLab):

- ρ_L^0 (on p) : $\approx 2.4 \times 10^4$

- ρ_L^+ : $\approx 1.5 \times 10^4$

- π^+ : $\approx 1.3 \times 10^4$

- ▶ **Small ξ study:**

With $160 < S_{\gamma N} < 20000$, probing $5 \cdot 10^{-5} < \xi < 5 \cdot 10^{-3}$:

- ρ_L^0 (on p) : $\approx 2.3 \times 10^3$

- ρ_L^+ : $\approx 1.8 \times 10^3$

- π^+ : $\approx 1.0 \times 10^3$

For p-Pb UPCs at LHC (integrated luminosity of 1200 nb^{-1}):

► With future data from runs 3 and 4,

– $\rho_L^0 : \approx 1.6 \times 10^4$

– $\rho_L^+ : \approx 1.0 \times 10^4$

– $\pi^+ : \approx 9.0 \times 10^3$

For p-Pb UPCs at LHC (integrated luminosity of 1200 nb^{-1}):

- ▶ With future data from runs 3 and 4,
 - $\rho_L^0 : \approx 1.6 \times 10^4$
 - $\rho_L^+ : \approx 1.0 \times 10^4$
 - $\pi^+ : \approx 9.0 \times 10^3$

- ▶ With $160 < S_{\gamma N} < 20000$, probing $5 \cdot 10^{-5} < \xi < 5 \cdot 10^{-3}$:
 - $\rho_L^0 : \approx 1.6 \times 10^3$
 - $\rho_L^+ : \approx 1.2 \times 10^3$
 - $\pi^+ : \approx 6.5 \times 10^2$

For p-Pb UPCs at LHC (integrated luminosity of 1200 nb^{-1}):

- ▶ With future data from runs 3 and 4,
 - $\rho_L^0 : \approx 1.6 \times 10^4$
 - $\rho_L^+ : \approx 1.0 \times 10^4$
 - $\pi^+ : \approx 9.0 \times 10^3$
- ▶ With $160 < S_{\gamma N} < 20000$, probing $5 \cdot 10^{-5} < \xi < 5 \cdot 10^{-3}$:
 - $\rho_L^0 : \approx 1.6 \times 10^3$
 - $\rho_L^+ : \approx 1.2 \times 10^3$
 - $\pi^+ : \approx 6.5 \times 10^2$
- ▶ Photon flux enhanced by a factor of Z^2 , but drops rapidly with $S_{\gamma N} \implies$ *Low luminosity not compensated by larger photon flux.*

- ▶ Exclusive photoproduction of photon-meson pair provides additional channel for extracting GPDs.

Conclusion

- ▶ Exclusive photoproduction of photon-meson pair provides additional channel for extracting GPDs.
- ▶ Especially interesting since it can probe chiral-odd GPD at the leading twist.

Conclusion

- ▶ Exclusive photoproduction of photon-meson pair provides additional channel for extracting GPDs.
- ▶ Especially interesting since it can probe chiral-odd GPD at the leading twist.
- ▶ Proof of factorisation for this family of processes now available.

Conclusion

- ▶ Exclusive photoproduction of photon-meson pair provides additional channel for extracting GPDs.
- ▶ Especially interesting since it can probe chiral-odd GPD at the leading twist.
- ▶ Proof of factorisation for this family of processes now available.
- ▶ Good statistics in various experiments, particularly at JLab.

Conclusion

- ▶ Exclusive photoproduction of photon-meson pair provides additional channel for extracting GPDs.
- ▶ Especially interesting since it can probe chiral-odd GPD at the leading twist.
- ▶ Proof of factorisation for this family of processes now available.
- ▶ Good statistics in various experiments, particularly at JLab.
- ▶ Small ξ limit of GPDs can be investigated by exploiting high energies available at EIC and UPCs at LHC.

- ▶ **Holographic** vs **Asymptotical** DA, **polarisation asymmetries** of incoming photon and kinematics for COMPASS, **EIC** and **LHC** at **UPC** [to appear!]

- ▶ **Holographic** vs **Asymptotical** DA, **polarisation asymmetries** of incoming photon and kinematics for COMPASS, **EIC** and **LHC** at **UPC** [to appear!]
- ▶ The processes $\gamma N \rightarrow \gamma \pi^0 N'$ and $\gamma N \rightarrow \gamma \eta^0 N'$ are of particular interest, since they give access to **gluonic** GPDs at Born level [ongoing]

- ▶ **Holographic** vs **Asymptotical** DA, **polarisation asymmetries** of incoming photon and kinematics for COMPASS, **EIC** and **LHC** at **UPC** [to appear!]
- ▶ The processes $\gamma N \rightarrow \gamma \pi^0 N'$ and $\gamma N \rightarrow \gamma \eta^0 N'$ are of particular interest, since they give access to **gluonic** GPDs at Born level [ongoing]
- ▶ Compute **NLO** corrections.

- ▶ **Holographic** vs **Asymptotical** DA, **polarisation asymmetries** of incoming photon and kinematics for COMPASS, **EIC** and **LHC** at **UPC** [to appear!]
- ▶ The processes $\gamma N \rightarrow \gamma \pi^0 N'$ and $\gamma N \rightarrow \gamma \eta^0 N'$ are of particular interest, since they give access to **gluonic** GPDs at Born level [ongoing]
- ▶ Compute **NLO** corrections.
- ▶ Generalise to **electroproduction** ($Q^2 \neq 0$).

- ▶ **Holographic** vs **Asymptotical** DA, **polarisation asymmetries** of incoming photon and kinematics for COMPASS, **EIC** and **LHC** at **UPC** [to appear!]
- ▶ The processes $\gamma N \rightarrow \gamma \pi^0 N'$ and $\gamma N \rightarrow \gamma \eta^0 N'$ are of particular interest, since they give access to **gluonic** GPDs at Born level [ongoing]
- ▶ Compute **NLO** corrections.
- ▶ Generalise to **electroproduction** ($Q^2 \neq 0$).
- ▶ Add **Bethe-Heitler** component (photon emitted from incoming lepton)
 - zero in chiral-odd case.
 - suppressed in chiral-even case.

- ▶ **Holographic** vs **Asymptotical** DA, **polarisation asymmetries** of incoming photon and kinematics for COMPASS, **EIC** and **LHC** at **UPC** [to appear!]
- ▶ The processes $\gamma N \rightarrow \gamma \pi^0 N'$ and $\gamma N \rightarrow \gamma \eta^0 N'$ are of particular interest, since they give access to **gluonic** GPDs at Born level [ongoing]
- ▶ Compute **NLO** corrections.
- ▶ Generalise to **electroproduction** ($Q^2 \neq 0$).
- ▶ Add **Bethe-Heitler** component (photon emitted from incoming lepton)
 - zero in chiral-odd case.
 - suppressed in chiral-even case.

The END

BACKUP SLIDES

What are GPDs?

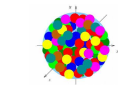
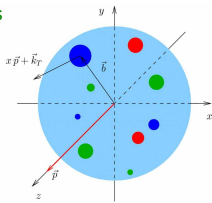
From Wigner distributions to GPDs and PDFs

6D/5D

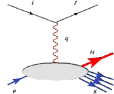
Wigner distributions
for hadrons

$$W(x, \vec{b}, k_T)$$

Experimentally
inaccessible directly



3D
perturbative Regge
limit



Semi-inclusive
processes

uPDFs (gluons)

Unintegrated parton
distributions

$$\int d^3 \vec{b}$$

TMDs

$$f(x, k_T)$$

Transverse momentum
dependent distributions

$$\int d^2 k_T \int d b_z$$

Impact parameter
distributions

$$f(x, b_T)$$

Impact parameter
distributions

$$b_T \leftrightarrow \Delta$$

$$H(x, 0, t)$$

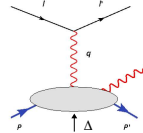
$$H(x, \xi, t)$$

$$t = -\Delta^2$$

$$\int d^2 k_T \int \text{Fourier}(\vec{b})$$

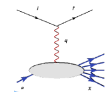
GPDs

generalised parton
distributions



exclusive
processes

1D



inclusive and semi-
inclusive processes

$$\int d^2 k_T$$

PDFs

$$f(x)$$

parton distributions

$$\int d^2 b_T$$



$t=0$



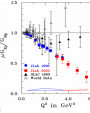
elastic processes

$$\int dx$$

FFs

$$G_{E,M}(t)$$

form factors



$$\int dx x^{n-1}$$

GFFs

generalized form factors

lattices

Computation

Parametrising the GPDs: ρ_L and π case, Chiral-even

$$\int \frac{dz^-}{4\pi} e^{ixP^+z^-} \langle p_2, \lambda_2 | \bar{\psi}_q \left(-\frac{1}{2}z^- \right) \gamma^+ \psi \left(\frac{1}{2}z^- \right) | p_1, \lambda_1 \rangle$$
$$= \frac{1}{2P^+} \bar{u}(p_2, \lambda_2) \left[H^q(x, \xi, t) \gamma^+ + E^q(x, \xi, t) \frac{i\sigma^{\alpha+} \Delta_\alpha}{2m} \right] u(p_1, \lambda_1)$$

$$\int \frac{dz^-}{4\pi} e^{ixP^+z^-} \langle p_2, \lambda_2 | \bar{\psi}_q \left(-\frac{1}{2}z^- \right) \gamma^+ \gamma^5 \psi \left(\frac{1}{2}z^- \right) | p_1, \lambda_1 \rangle$$
$$= \frac{1}{2P^+} \bar{u}(p_2, \lambda_2) \left[\tilde{H}^q(x, \xi, t) \gamma^+ \gamma^5 + \tilde{E}^q(x, \xi, t) \frac{\gamma^5 \Delta^+}{2m} \right] u(p_1, \lambda_1)$$

- ▶ Take the limit $\Delta_\perp = 0$.
- ▶ In that case and for small ξ , the dominant contributions come from H^q and \tilde{H}^q .

Computation

Parametrising the GPDs: ρ_T case, Chiral-odd

$$\begin{aligned} & \int \frac{dz^-}{4\pi} e^{ixP^+z^-} \langle p_2, \lambda_2 | \bar{\psi}_q \left(-\frac{1}{2}z^- \right) i\sigma^{+i} \psi \left(\frac{1}{2}z^- \right) | p_1, \lambda_1 \rangle \\ &= \frac{1}{2P^+} \bar{u}(p_2, \lambda_2) \left[H_T^q(x, \xi, t) i\sigma^{+i} + \tilde{H}_T^q(x, \xi, t) \frac{P^+ \Delta^i - \Delta^+ P^i}{M_N^2} \right. \\ &+ \left. E_T^q(x, \xi, t) \frac{\gamma^+ \Delta^i - \Delta^+ \gamma^i}{2M_N} + \tilde{E}_T^q(x, \xi, t) \frac{\gamma^+ P^i - P^+ \gamma^i}{M_N} \right] u(p_1, \lambda_1) \end{aligned}$$

- ▶ Take the limit $\Delta_\perp = 0$.
- ▶ In that case and for small ξ , the dominant contributions come from H_T^q .

- ▶ GPDs can be represented in terms of **Double Distributions** [Radyushkin]

$$H^q(x, \xi, t = 0) = \int_{-1}^1 d\beta \int_{-1+|\beta|}^{1-|\beta|} d\alpha \delta(\beta + \xi\alpha - x) f^q(\beta, \alpha)$$

- ▶ ansatz for these Double Distributions [Radyushkin]:

- ▶ chiral-even sector:

$$\begin{aligned} f^q(\beta, \alpha, t = 0) &= \Pi(\beta, \alpha) q(\beta) \Theta(\beta) - \Pi(-\beta, \alpha) \bar{q}(-\beta) \Theta(-\beta), \\ \tilde{f}^q(\beta, \alpha, t = 0) &= \Pi(\beta, \alpha) \Delta q(\beta) \Theta(\beta) + \Pi(-\beta, \alpha) \Delta \bar{q}(-\beta) \Theta(-\beta). \end{aligned}$$

- ▶ chiral-odd sector:

$$f_T^q(\beta, \alpha, t = 0) = \Pi(\beta, \alpha) \delta q(\beta) \Theta(\beta) - \Pi(-\beta, \alpha) \delta \bar{q}(-\beta) \Theta(-\beta).$$

- ▶ $\Pi(\beta, \alpha) = \frac{3}{4} \frac{(1-\beta)^2 - \alpha^2}{(1-\beta)^3}$: profile function

- ▶ simplistic factorised ansatz for the t -dependence:

$$H^q(x, \xi, t) = H^q(x, \xi, t = t_{\min}) \times F_H(t)$$

with $F_H(t) = \frac{(t_{\min} - C)^2}{(t - C)^2}$ a standard **dipole form factor**
($C = 0.71 \text{ GeV}^2$)

- ▶ $q(x)$: unpolarized PDF [GRV-98]
and [MSTW2008lo, MSTW2008nnlo, ABM11nnlo, CT10nnlo]
- ▶ $\Delta q(x)$ polarized PDF [GRSV-2000]
- ▶ $\delta q(x)$: transversity PDF [Anselmino *et al.*]

Effects are not significant! But relevant for NLO corrections!

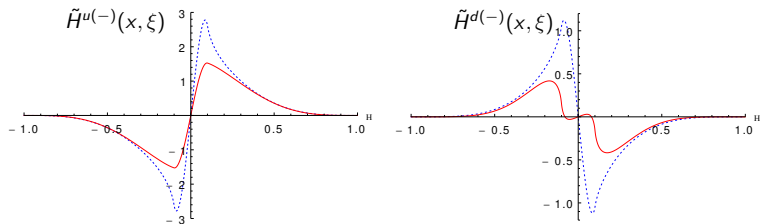
Computation

Valence vs Standard scenarios in \tilde{H} (Chiral-even, Axial)

Typical kinematic point (for JLab kinematics):

$$\xi = .1 \leftrightarrow S_{\gamma N} = 20 \text{ GeV}^2 \text{ and } M_{\gamma\rho}^2 = 3.5 \text{ GeV}^2$$

$$\tilde{H}^{q(-)}(x, \xi, t) = \tilde{H}^q(x, \xi, t) - \tilde{H}^q(-x, \xi, t) \quad [C = -1]$$



“valence” and “standard”: two GRSV Ansätze for $\Delta q(x)$

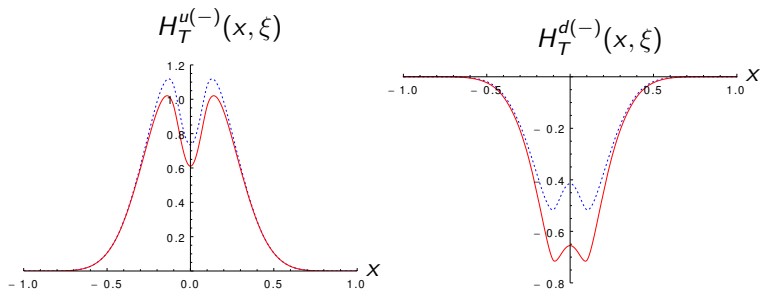
Computation

Valence vs Standard scenarios in H_T (Chiral-odd)

Typical kinematic point (for JLab kinematics):

$$\xi = .1 \leftrightarrow S_{\gamma N} = 20 \text{ GeV}^2 \text{ and } M_{\gamma\rho}^2 = 3.5 \text{ GeV}^2$$

$$H_T^{q(-)}(x, \xi, t) = H_T^q(x, \xi, t) + H_T^q(-x, \xi, t) \quad [C = -1]$$



“valence” and “standard”: two GRSV Ansätze for $\Delta q(x)$

\Rightarrow two Ansätze for $\delta q(x)$

- Helicity conserving (vector) DA at twist 2: ρ_L

$$\langle 0 | \bar{u}(0) \gamma^\mu u(x) | \rho^0(p, s) \rangle = \frac{p^\mu}{\sqrt{2}} f_\rho \int_0^1 du e^{-iup \cdot x} \phi_{\parallel}(u)$$

- ρ_T DA at twist 2:

$$\langle 0 | \bar{u}(0) \sigma^{\mu\nu} u(x) | \rho^0(p, s) \rangle = \frac{i}{\sqrt{2}} (\epsilon_\rho^\mu p^\nu - \epsilon_\rho^\nu p^\mu) f_\rho^\perp \int_0^1 du e^{-iup \cdot x} \phi_\perp(u)$$

- ▶ Work in the limit of:

- $\Delta_{\perp} \ll p_{\perp}$
- $M^2, m_{\rho}^2 \ll M_{\gamma\rho}^2$

- ▶ initial state particle momenta:

$$q^{\mu} = n^{\mu},$$

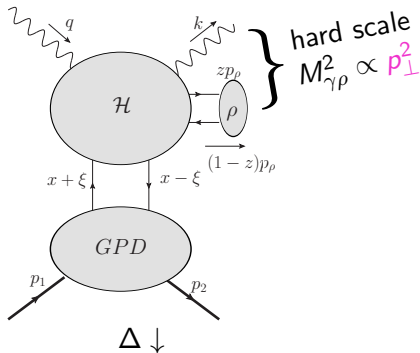
$$p_1^{\mu} = (1 + \xi) p^{\mu} + \frac{M^2}{s(1+\xi)} n^{\mu}$$

- ▶ final state particle momenta:

$$p_2^{\mu} = (1 - \xi) p^{\mu} + \frac{M^2 + \vec{p}_t^2}{s(1 - \xi)} n^{\mu} + \Delta_{\perp}^{\mu}$$

$$k^{\mu} = \alpha n^{\mu} + \frac{(\vec{p}_t - \vec{\Delta}_t/2)^2}{\alpha s} p^{\mu} + p_{\perp}^{\mu} - \frac{\Delta_{\perp}^{\mu}}{2},$$

$$p_{\rho}^{\mu} = \alpha_{\rho} n^{\mu} + \frac{(\vec{p}_t + \vec{\Delta}_t/2)^2 + m_{\rho}^2}{\alpha_{\rho} s} p^{\mu} - p_{\perp}^{\mu} - \frac{\Delta_{\perp}^{\mu}}{2},$$

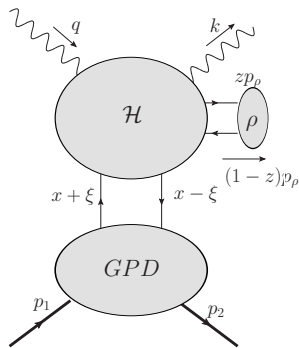


$$\mathcal{A} \propto \int_{-1}^1 dx \int_0^1 dz T(x, \xi, z) H(x, \xi, t) \Phi_\rho(z)$$

- ▶ z integration performed **analytically** using an asymptotic or holographic DA.
- ▶ GPD models plugged into expression for amplitude and the integral performed w.r.t. x **numerically**.
- ▶ Differential cross section:

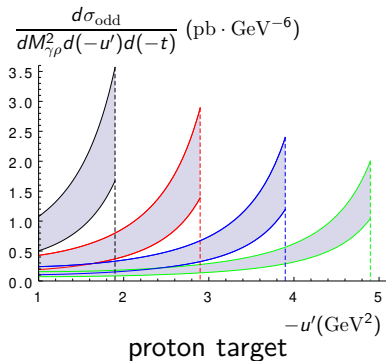
$$\left. \frac{d\sigma}{dt du' dM_{\gamma\rho}^2} \right|_{-t=(-t)_{min}} = \frac{|\overline{\mathcal{A}}|^2}{32 S_{\gamma N}^2 M_{\gamma\rho}^2 (2\pi)^3} \cdot$$

- ▶ Kinematic parameters: $S_{\gamma N}$, $M_{\gamma\rho}^2$ and $-u'$
Recall: $u' = (p_\rho - q)^2$, $t = (p_2 - p_1)^2$

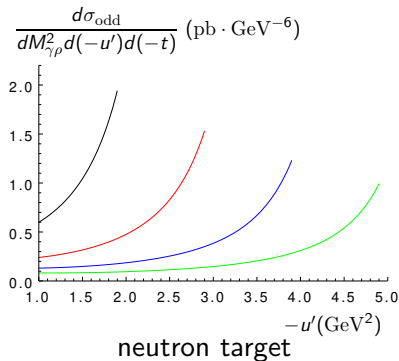


Results

Fully-differential cross-sections: ρ_T^0 (Chiral odd)



“valence” and “standard” models,
each of them with $\pm 2\sigma$ [S. Melis]



“valence” model only

$$S_{\gamma N} = 20 \text{ GeV}^2 \text{ at } -t = (-t)_{\text{min}}$$

$$M_{\gamma\rho}^2 = 3, 4, 5, 6 \text{ GeV}^2$$

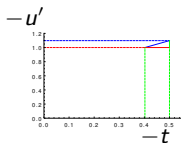
Results

Phase space integration: Evolution in $(-t, -u')$ plane

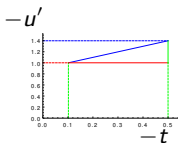
large angle scattering: $M_{\gamma\rho}^2 \sim -u' \sim -t'$

$\Rightarrow -u' > 1 \text{ GeV}^2$ and $-t' > 1 \text{ GeV}^2$ and $(-t)_{\min} \leq -t \leq .5 \text{ GeV}^2$

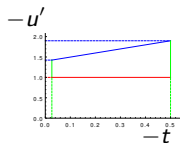
example: $S_{\gamma N} = 20 \text{ GeV}^2$



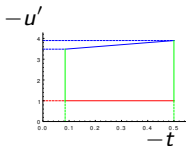
$$M_{\gamma\rho} = 2.2 \text{ GeV}^2$$



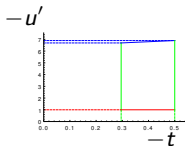
$$M_{\gamma\rho} = 2.5 \text{ GeV}^2$$



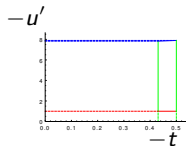
$$M_{\gamma\rho} = 3 \text{ GeV}^2$$



$$M_{\gamma\rho} = 5 \text{ GeV}^2$$



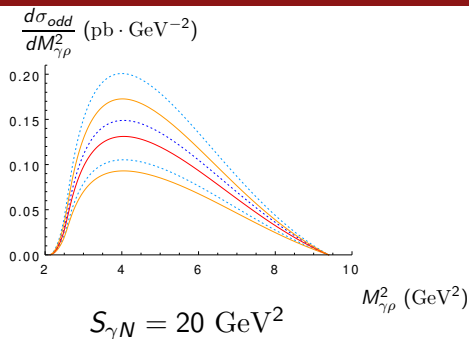
$$M_{\gamma\rho} = 8 \text{ GeV}^2$$



$$M_{\gamma\rho} = 9 \text{ GeV}^2$$

Results

Single differential cross-section: Valence vs Standard: ρ_T (Chiral odd)

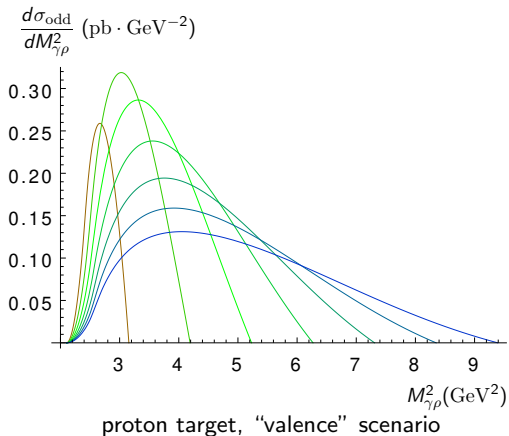


Various ansätze for the PDFs Δq used to build the GPD H_T :

- ▶ *dotted curves*: “standard” scenario
- ▶ *solid curves*: “valence” scenario
- ▶ *deep-blue* and *red* curves: central values
- ▶ *light-blue* and *orange*: results with $\pm 2\sigma$.

Results

Single differential cross-section: ρ_T^0 (Chiral odd)



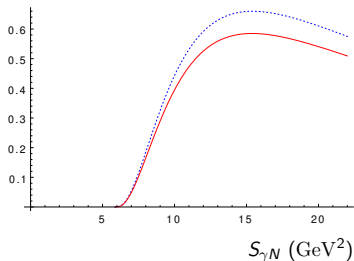
$$S_{\gamma N} = 8, 10, 12, 14, 16, 18, 20 \text{ GeV}^2$$

typical JLab kinematics

Results

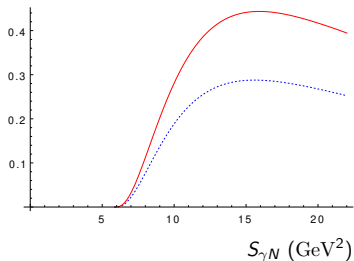
Integrated cross-section: Valence vs Standard: ρ_T^0 (Chiral odd)

σ_{odd} (pb)



proton target

σ_{odd} (pb)



neutron target

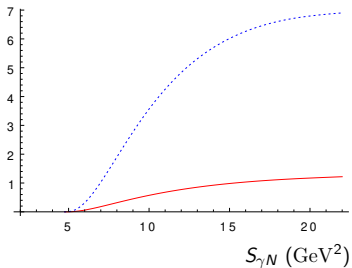
solid red: "valence" scenario

dashed blue: "standard" one

Results

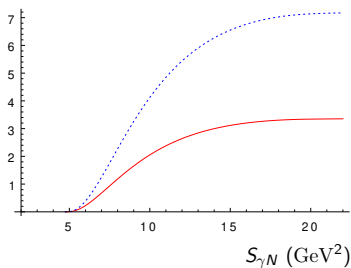
Integrated cross-section: Valence vs Standard: π^\pm (Chiral even)

$\sigma_{\gamma\pi^+}$ (pb)



proton target

$\sigma_{\gamma\pi^-}$ (pb)



neutron target

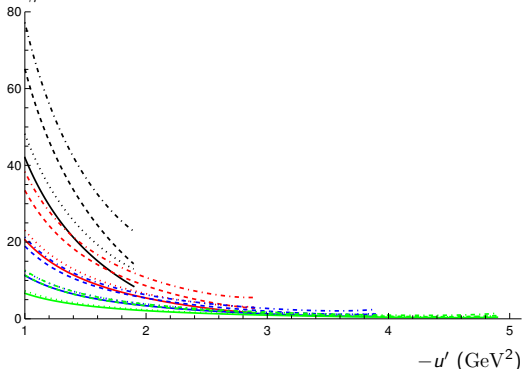
solid red: "valence" scenario

dashed blue: "standard" one

Results (Preliminary)

Fully differential X-section: Holographic DA vs Asymptotical DA: ρ_L^0 , Chiral-even

$$\frac{d\sigma_{\text{even}}}{dM_{\gamma\rho}^2 d(-u') d(-t)} \text{ (pb} \cdot \text{GeV}^{-6}\text{)}$$



dashed dotted:

Hol. DA, “standard” model

dashed:

Hol. DA, “valence” model

dotted:

Asymp. DA, “standard” model

solid:

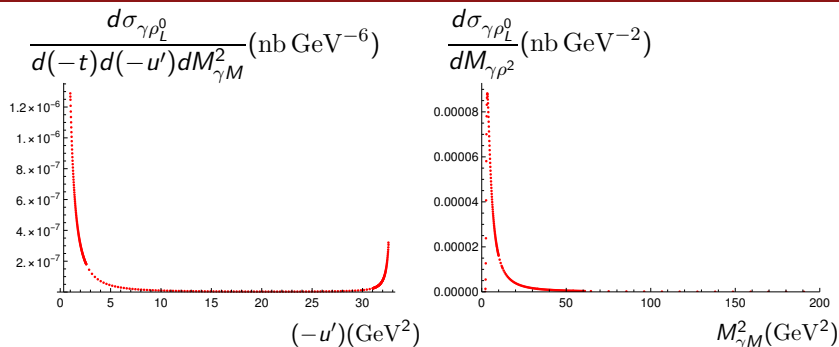
Asymp. DA, “valence” model

$$S_{\gamma N} = 20 \text{ GeV}^2, \text{ at } -t = (-t)_{\text{min}}$$

$$M_{\gamma\rho}^2 = 3, 4, 5, 6 \text{ GeV}^2$$

⇒ sizable effect, larger than the one due to uncertainties on polarized PDFs

Necessity for Importance Sampling

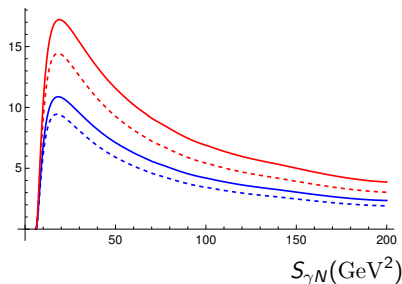


- ▶ Need enough points at boundaries for distribution in $(-u')$
- ▶ Need enough points to resolve peak (at low $M_{\gamma M}^2$) for distribution in $M_{\gamma M}^2$

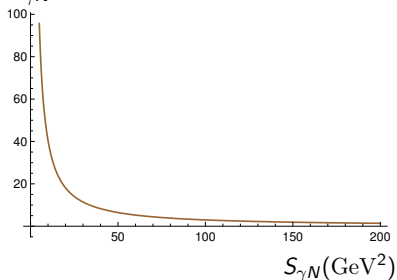
Prospects at experiments

Why counting rates lower UPCs at LHC?

$\sigma_{\gamma\rho_L^0}$ (pb)



$\frac{dN_\gamma}{dS_{\gamma N}}$ (GeV^{-2})



Hol. DA vs Asymp. DA Solid: standard vs Dashed: valence

- ▶ LHC great for high energy, but JLab better in terms of luminosity.
- ▶ Still, LHC gives us access to the small ξ region of GPDs!

Circular asymmetry of incoming photon

Why does it vanish for unpolarised target?

Consider

$$\gamma(q, \lambda_q) + N(p_1, \lambda_1) \rightarrow \gamma(k, \lambda_k) + \rho^0(p_\rho, \varepsilon_\rho) + N'(p_2, \lambda_2),$$

where λ_i represent the helicities of the particles.

QED/QCD **invariance under parity** implies that [Bourrely, Soffer, Leader]

$$\mathcal{A}_{\lambda_2 \lambda_k; \lambda_1 \lambda_q} = \eta (-1)^{\lambda_1 - \lambda_q - (\lambda_2 - \lambda_k)} \mathcal{A}_{-\lambda_2 - \lambda_k; -\lambda_1 - \lambda_q},$$

where η represents phase factors related to intrinsic spin.

Thus, at the cross-section level, it is clear that circular asymmetry will vanish, since

$$\sum_{\lambda_i, i \neq q} |\mathcal{A}_{\lambda_2 \lambda_k; \lambda_1 +}|^2 = \sum_{\lambda_i, i \neq q} |\mathcal{A}_{\lambda_2 \lambda_k; \lambda_1 -}|^2$$